Sains Malaysiana 53(10)(2024): 3487-3497
http://doi.org/10.17576/jsm-2024-5310-21

Automatic Algorithm Applied for Calculating Thermal Conductivity by Transient Plane Source Method

(Algoritma Automatik Digunakan untuk Menghitung Kekonduksian Terma melalui Kaedah Sumber Satah Fana)

ZHIJIE JIA[1,2], LIPING YANG[2,3], CHENGCHENG CAO[2], HUIDONG LI[2], CAIYUN LUO[2], YE TAO[2], QIU ZHONG[2], ZIJUN XU[2], ZEZHONG CHEN[1],*

[1]*School of Materials Science and Engineering, University of Shanghai for Science and Technology, Shanghai 200093, China*
[2]*Inorganic Materials Analysis and Testing Center, Shanghai Institute of Ceramics, Chinese Academy of Sciences, Shanghai 200050, China*
[3]*State Key Laboratory of High-Performance Ceramics and Superfine Microstructure, Shanghai Institute of Ceramics, Chinese Academy of Sciences, Shanghai 200050, China*

Received: 14 March 2024/Accepted: 13 August 2024

ABSTRACT

As a thermal conductivity measurement method, Transient Plane Source (TPS) method has gained much popularity because of its broad applicability, short measurement times, high precision and simple sample preparation. However, the accuracy of thermal conductivity calculations based on temperature rise data is often hindered by factors such as probe thickness, contact thermal resistance, and input power. Currently, there is no standardized criteria for selecting effective temperature rise data for thermal conductivity calculation. Consequently, the accuracy of results are limited by the operator's understanding of the TPS methods, and repeatability of the results is often poor. To address this issue, an automatic algorithm based on the international standard (ISO22007-2:2008) is proposed in this paper. By applying this algorithm to the measurement of different materials, it has been demonstrated that the proposed algorithm can produce more precise and consistent results than the conventional method. Additionally, the integration of the time window function t_{max} / θ, typically utilized solely for result validation in conventional methods, further enhances the objectivity and reproducibility of the results obtained by the automatic algorithm

Keywords: Linear regression analysis; thermal conductivity; the effective measurement interval; transient plane source method

ABSTRAK

Sebagai kaedah pengukuran kekonduksian terma, kaedah Sumber Satah Fana (TPS) telah mendapat populariti kerana kebolehgunaannya yang luas, masa pengukuran yang singkat, ketepatan tinggi dan penyediaan sampel yang mudah. Walau bagaimanapun, ketepatan pengiraan kekonduksian terma berdasarkan data kenaikan suhu sering dihalang oleh faktor seperti ketebalan prob, rintangan terma sentuhan dan kuasa input. Pada masa ini, tiada kriteria piawai untuk memilih data kenaikan suhu yang berkesan untuk pengiraan kekonduksian terma. Akibatnya, ketepatan keputusan dihadkan oleh pemahaman pengendali tentang kaedah TPS, dan kebolehulangan keputusan selalunya lemah. Untuk menangani isu ini, algoritma automatik berdasarkan piawaian antarabangsa (ISO22007-2:2008) dicadangkan dalam kertas ini. Dengan menggunakan algoritma ini untuk pengukuran bahan yang berbeza, ia telah menunjukkan bahawa algoritma yang dicadangkan boleh menghasilkan keputusan yang lebih tepat dan tekal berbanding kaedah konvensional. Selain itu, penyepaduan fungsi tetingkap masa t_{max} / θ, biasanya digunakan semata-mata untuk pengesahan keputusan dalam kaedah konvensional, meningkatkan lagi objektiviti dan kebolehulangan hasil yang diperoleh oleh algoritma automatik.

Kata kunci: Analisis regresi linear; kaedah sumber satah fana; kekonduksian terma; selang pengukuran berkesan

INTRODUCTION

Thermal conductivity is a very important thermal physical property parameter to measure heat transfer capacity of materials, which plays an important role in the fields of construction, machinery, and energy. The present measurement methods available for thermal conductivity can be divided into two categories: steady state method (Xamán, Lira & Arce 2009) and unsteady state method (Cahill 1990; Lian et al. 2016; Zhao et al. 2020).

The TPS (Ai et al. 2016; Gustafsson 1991; Gustavsson, Karawacki & Gustafsson 1994) is a thermal conductivity measurement method developed by Professor Gustafsson in 1981 based on the Transient Hot Wire (THW) method (Assael, Antoniadis & Wakeham 2010; Assael, Antoniadis & Tzetzis 2008; Assael et al. 2002). It is classified as an unsteady state method, also known as 'Hot Disk'. An international standard has been established for this method (ISO22007-2:2008) (ISO 2008 Plastics—determination of thermal conductivity and thermal diffusivity—part 2: transient plane heat source (hot disc) method ISO 22007-2 (Geneva: ISO)). The TPS method has gained much popularity because of its wide range, short time, high precision and simple sample preparation. On the one hand, this method can be applied to the measurement of thermal insulation (Almanza, Rodríguez-Pérez & De Saja 2004; Ma et al. 2021; Zheng et al. 2020), porous (Mo et al. 2006), liquid (Warzoha & Fleischer 2014a, 2014b), anisotropic (Elkholy, Sadek & Kempers 2019; Zhang, Li & Tao 2017), interface (Wang et al. 2019) and other materials. On the other hand, it can be applied to the measurement of high temperature, microgravity (Nagai, Mamiya & Okutani 2007) and other environments. Therefore, many researchers have revised and improved the present theoretical model. Huang and Liu (2009) simplified the originally complex dimensionless time function in the formula into a power function polynomial by sampling point fitting, which greatly simplified the calculation process. Li et al. (2014) further improved the measurement accuracy by correcting the deviation caused by the heat capacity and power instability of the probe. Zhang et al. (2013) explored the insulation layer of the probe on measurement accuracy through numerical analysis.

Although many researchers have improved the TPS method in various aspects, determining the effective measurement interval for calculating thermal conductivity is still a challenging issue. In the conventional method, the initial detection time $t_{\min}$ is determined by considering the influence of the insulation layer, but ignoring the influence of probe thickness, contact thermal resistance, and input power, which ultimately leads to poor repeatability of the measurement result. Bohac et al. (2000) has proposed a time window function $t_{\max}/\theta$ through sensitivity analysis of thermal conductivity and thermal diffusivity, which helps determine the maximum measurement time $t_{\max}$. However, the thermal diffusivity within the time window $t_{\max}/\theta$ function is also a value to be measured, so it can only serve as a means to validate the measurement results rather than directly contributing to the measurement process.

In view of the challenge of selecting the effective temperature rise data for calculating thermal conductivity in TPS method. Based on the relevant international standard (ISO22007-2:2008), an automatic algorithm is proposed in this paper to calculate thermal conductivity, which divides the temperature rise curve into three intervals by analyzing the coefficient of determination (R^2) (Kim, Lee & Koo 2019) between temperature rise data and time: The disturbed interval, and the effective measurement interval, the ineffective measurement interval. Then, the time window function $t_{\max}/\theta$ is used to narrow the calculation range again in the effective measurement interval, and the preliminary thermal conductivity array is obtained. Finally, the obtained thermal conductivity array is grouped and analyzed, with separate calculations for the average and standard deviation of each group. The mean value of the group with the smallest standard deviation is the final measurement. The feasibility of the algorithm is verified by the measurement of glass materials (ordinary glass, quartz glass, neodymium glass), thermal silica gel and stainless-steel.

THEORY OF THE TRANSIENT PLANE SOURCE METHOD

The probe is the core of TPS method, serving as both heat source and thermometer in the measurement process, its structure shown in Figure 1(a). Considering the change of its use environment, the covering insulation layer is generally made of polyimide, mica, alumina, aluminum nitride and other materials (Malinarič & Dieška 2015). The sensor is sandwiched between two solid samples or immersed in a fluid during measurement to comply with the hypothesis in TPS theory regarding heat transfer in a semi-infinite medium from a concentric ring heat source. The heat transfer model is shown in Figure 1(b).

The temperature change of the sensor is calculated according to its resistance change, and the measurement principle diagram is shown in Figure 2, and the formula is as follows

$$R(t) = R_0[1+\alpha\Delta\overline{T}(\tau)] \tag{1}$$

where $R(t)$ represents the resistance value of the probe at time t; R_0 is the temperature coefficient (TCR) of the probe; $\Delta\overline{T}(\tau)$ is the surface average temperature rise of the sample.

In Equation (1), the average temperature rise $\Delta\overline{T}(\tau)$ is expressed as a function of dimensionless time τ ,where τ defined as:

$$\tau = \sqrt{\frac{t}{\theta}},\quad \theta = \frac{a^2}{k} \tag{2}$$

where θ is the characteristic time; t is the measurement time in unit of s; a is the average radius of the probe's outermost ring in i of mm; k is the thermal diffusivity of the sample in units of $mm^2 \cdot s^{-1}$.

It should be noted that the constant power should be applied to the probe during the measurement process. The formula for the temperature change of the probe is defined as (Gustafsson 1991)

$$\Delta T(\tau) = \frac{P_0}{\pi^{\frac{3}{2}} a\lambda} D(\tau) \tag{3}$$

where P_0 is the constant power applied in unit of W; λ is the thermal conductivity of the sample in unit of Wm-1K-1;

and $D(\tau)$ is a dimensionless time function about τ which defined as

$$D(\tau)=\frac{1}{m^2(m+1)^2}\int_0^{2\pi}\sigma^{-2}\left[\sum_i^m i\sum_l^m l\exp\left(\frac{l^2+i^2}{4m^2\sigma^2}\right)I_0\left(\frac{li}{2m^2\sigma^2}\right)\right]d\sigma \quad (4)$$

where σ^2 is proposed to simplify the calculation formula, which defined as

$$\sigma^2=\frac{k(t-t^{'})}{a^2} \quad (5)$$

where m is the number of coils; $t^{'}$ represents the time delay caused by equipment delay; $I_0(x)$ is the first Bessel correction function defined as follows

$$I_0(x)=\frac{1}{2\pi}\int_0^{2\pi}e^{x\cos\theta}d\theta=\frac{1}{2\pi}\int_0^{2\pi}e^{x\sin\theta}d\theta \quad (6)$$

From this analysis, the calculation of sample thermal conductivity needs the following steps: Firstly, the curve of temperature rise with time is recorded. Secondly, the correlation coefficient between $\Delta T(\tau)$ and $D(\tau)$ is optimized by iterating the thermal diffusivity k, and the slope between them can be obtained by the least square method in the iterative process. Finally, the k can be obtained at the last step of the iteration, and λ is determined by the slope.

ALGORITHM IMPROVEMENT

In the conventional TPS measurement method, when choosing the data for calculating thermal conductivity, the initial detection time $t_{\min}$ is determined by the influence of the insulation layer, and the maximum detection time $t_{\max}$ is determined by the time window function $t_{\max}/\theta$ (Bohac et al. 2000). Additionally, it is necessary to avoid its detection depth exceeding the detectable depth Δp.The initial detection time $t_{\min}$ is defined as

$$t_{\min}=\frac{\delta^2}{k_S} \quad (7)$$

where δ is the thickness of the insulation layer. and k_S is the thermal diffusivity of the insulation layer.The detectable depth is defined as

$$\Delta p=2\sqrt{kt_{tot}} \quad (8)$$

where t_{tot} is the total measurement time.

However, in actual measurement, the thermal diffusivity within Equations (7) and (8) also represents the value to be measured. In addition, it is not sufficient to take into account only the theoretical temperature rise of the insulation layer. The thickness of the probe, contact thermal resistance and input power also significantly influence the selection of the temperature rise data for calculating the thermal conductivity.

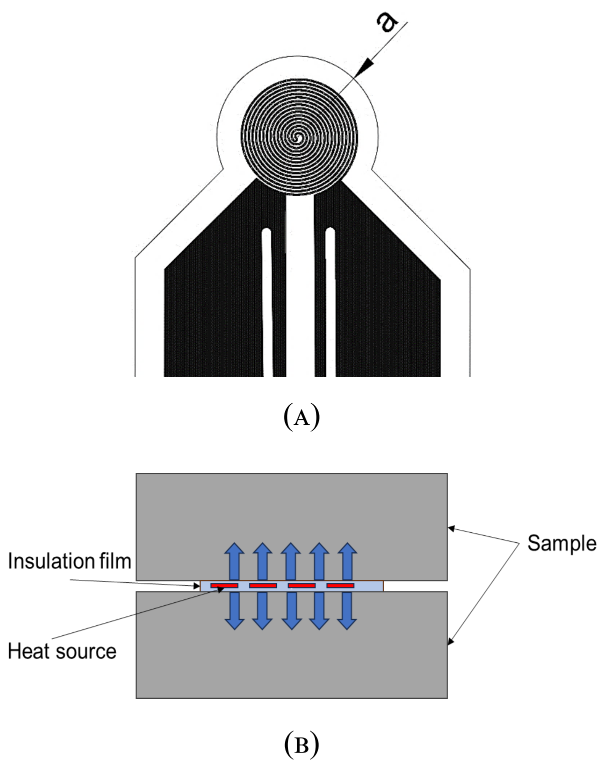

FIGURE 1. (a) Structure of the probe, and (b) Sample placement

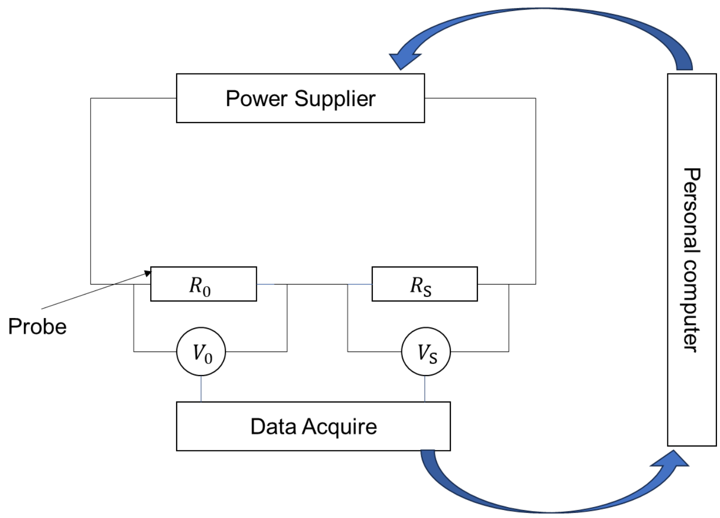

FIGURE 2. Measurement principle diagram of TPS method

Figure 3 shows an automatic algorithm applied to the TPS method, which is divided into three steps: (1) Obtaining temperature rise data; (2) Determining the calculation range and getting the thermal conductivity array; (3) Grouping the array for analysis in order to determine the final measurement value.

Step (1) Parameters such as voltage E, sampling rate Δt, total measurement time t_{tot} and the resistance temperature coefficient α are input. The collected voltage signals are then converted into temperature rise signals, resulting in a data volume of N. To ensure calculation accuracy, N should be greater than or equal to 100.

Step (2) the effective measurement interval is determined by the temperature rise resolution recommended by standard (ISO22007-2:2008) and its linear correlation with time. Subsequently, the time window function $t_{\max}/\theta$ is used to narrow the calculation range again. Finally, the preliminary thermal conductivity array is obtained by iterative calculation. The specific order is as follows: Firstly, the length of the temperature rise data, used for calculating thermal conductivity is determined X points, with X range is $[100, N]$ to ensure accuracy. It is necessary to make sure that the time corresponding to the first temperature rise data point t_m exceeds the initial detection time $t_{\min}$.

Secondly, the linear and the resolution of the temperature rise signals analysis of the firstly selected data are carried out. Linear analysis assumes a constant power applied to the probe, indicating that the temperature rise signal curve should exhibit a linear relationship with time. However, factors such as probe thickness, contact thermal resistance, and input power often lead to poor linearity at the initial interval of the curve. Therefore, this interval can be classified as a disturbance interval. When selecting the data for calculation, according to variation in the thermal conductivity of the tested materials, the algorithm proposed in this paper retains only the data of $R^2 \geq [0.95, 0.995]$.

The analysis of resolution of the temperature rise signal depends on the fact that the selected data used for calculating the thermal conductivity should reflect the change of thermodynamic state. However, with the extension of time, the channels for heat propagation widen, the temperature rise curve gradually flattens out and the resolution gradually decreases (Elkholy, Sadek & Kempers 2019). Therefore, it is classified as the ineffective measurement interval and should be excluded, if the resolution ($\Delta\overline{T}(t)$) of the temperature rise signals in the selected interval is lower than the recommended value ($\Delta\overline{T}_{STD}(t)$) established by the standard (ISO22007-2:2008).

Thirdly, the retained data is iteratively calculated, and the results of each iteration are verified by the time window function, Based on sensitivity analysis of thermal diffusivity and thermal conductivity (Bohac et al. 2000), when the $t_{\max}/\theta$ is [0.3,1.0] can get more accurate thermal conductivity. Subsequently, the thermal conductivity array is obtained. It should be noted that in order to reduce the impact of power fluctuations and heat loss caused by probe heat capacity, a power correction module (Li et al. 2014) is introduced in the iterative process. Figure 4 shows the temperature rise curve of the stainless-steel sample at room temperature. When the input power is 2.5W, it can be seen that the total measurement time is 15s, the effective measurement interval of measurement is from 1.88 to 11.92s, accounting for 66.95% of the total measurement time.

Step (3) The degree of dispersion of the preliminary array collected in Step 2 is analyzed. During the analysis, it is necessary to divide the thermal conductivity array into groups, each with a length of j, and calculate the standard deviation and mean value for each group. The mean value of the group with the smallest standard deviation is the final measurement result.

EXPERIMENTAL INSTRUMENTS AND MATERIALS

In this experiment, the probe is a 16-turn nickel wire coil, the structure is shown in Figure 1(a), the radius is 6.9 mm, and the resistance is 13.6 Ω at room temperature. During the measurement, the probe is sandwiched between two samples to form the structure shown in Figure 1(b). The power is provided by Agilent E3632A DC power supply, the data acquisition is completed by Fluke1586A, and the fixed resistance R_s is controlled by a resistance box (ZX74 DC resistance box, produced by Shanghai Dongmao Electronic Technology Co., LTD.), the measurement scheme is shown in Figure 2. Five materials are measured at room temperature to verify the algorithm shown in Figure 3. The test samples are neodymium glass ($\lambda_{THW} = 0.956$ Wm-1K-1), ordinary glass ($\lambda_{THW} = 1.156$Wm-1K-1), quartz glass (produced by Kyoto electronic Company, the calibration value $\lambda_0 = 1.428$ Wm-1K-1), heat dissipation silicone grease ($\lambda_{THW} = 2.215$ Wm-1K-1) and stainless-steel (produced by NIST, the calibration value ($\lambda_0 = 14.2$Wm-1K-1). The reference values λ_{THW} are acquired by QTM-500(A Quick Thermal Conductivity Meter produced by Tokyo Electronic). The specific experimental parameters of the five materials are shown in Table 1.

RESULTS AND DISCUSSIONS

The main idea of the experiment is as follows: Firstly, apply different power to the stainless-steel standard sample, observe the change in the temperature rise interval, and gain an intuitive understanding of the working principle of the algorithm. Secondly, the advantages of the algorithm are demonstrated by comparing with the conventional method. Finally, five kinds of materials with different thermal conductivity are measured, and the change of their measurement results with respect to power is observed, which further proves the superiority and stability of the algorithm.

HOW THE ALGORITHM WORKS

The core of the algorithm is the division and selection of the temperature rise interval used to calculate the thermal conductivity. Figure 5 shows the division of the measurement interval of stainless-steel under different powers, it is evident that the effective temperature rise interval in the temperature rise curve increases with the increase of power. On the one hand, this can be attributed to the decrease in heat loss caused by factors such as probe thickness and contact thermal resistance as power increases, leading to a decrease in the proportion of the disturbed interval. On the other hand, the resolution of the temperature rise signal increases with the increase in power, leading to a decrease in the proportion of the ineffective measurement interval. Therefore, in traditional methods, the measurement accuracy increases with the increase of power (Huang 2007). This is because as the power increases, the probability of selecting the data used to calculate the thermal conductivity within the effective measurement interval also increases. Table 2 shows the change of the proportion of the measurement intervals for stainless-steel with respect to power. As the power increases from 2.1 to 4.0W, the proportion of the effective measurement interval also increases from 60% to 87.8%.

VALIDITY TEST OF ALGORITHM

Figure (6) shows the results of measuring a stainless-steel standard sample using both the automatic method and the conventional method under three different power levels, and each measurement comprises 20 sets. The advantage of the algorithm is demonstrated by analyzing the mean value and the degree of the dispersion of the two sets of data. It is important to note that the time of the first point for two calculation methods needs to exceed the $t_{\min}$ (which is 0.05s in this paper).

Figure 6(a) shows that when the input power is 2.1W, for the automatic method, the thermal conductivity is measured 13.899±0.003Wm-1K-1 with a deviation of 2.6% from the reference value. In contrast, for the conventional method, the measured value is 11.398±4.890Wm-1K-1 with a deviation of 9%. It is evident that the automatic method is superior to the traditional method both in accuracy and stability.

The distribution of Figure 6(b) and Figure 6(c) is consistent with that of Figure 6(a). When the input power is 2.5W, for the automatic method, the measured value is 13.888±0.0025Wm-1K-1 with a deviation of 2.6% for the conventional method, the measured value is 11.038±4.797Wm-1K-1 with a deviation of 7.4%. When the input power is 3.0W, for the automatic method, the measured value is 14.035±0.004 Wm-1K-1 with a deviation of 1.1%, for the conventional method, the measured value is 11.139±5.361Wm-1K-1 with a deviation of 8.3%.

From these three groups of comparison, it can be concluded that compared with the traditional method, in addition to higher accuracy and stability, the measurement results of the automatic method also vary slightly with power. As the power increases from 2.1W to 3.0W, for the automatic method, the thermal conductivity is measured 13.962±0.074Wm-1K-1, and for the traditional method, the thermal conductivity is measured 13.037±0.116Wm-1K-1. This will be further confirmed in the following experiment.

MEASUREMENT RESULTS OF DIFFERENT MATERIALS

Figure 7 shows the thermal conductivity distribution for five materials with different power levels. In Figure 6(a), three glass materials are presented, Figure 7(b) presents thermal dissipation silicone grease, and Figure 7(c) is

TABLE 1. Measured sample and set parameters

Material	Power/W	Total measurement time/s	Sampling frequency/s	Temperature/°C
Neodymium glass				
Ordinary glass	0.3 - 1.3	60	0.2	
Quartz glass				Room temperature
Heat dissipation silicone grease	0.4 - 1.3	40	0.2	
Stainless-steel	1.5 - 5.5	15	0.04	

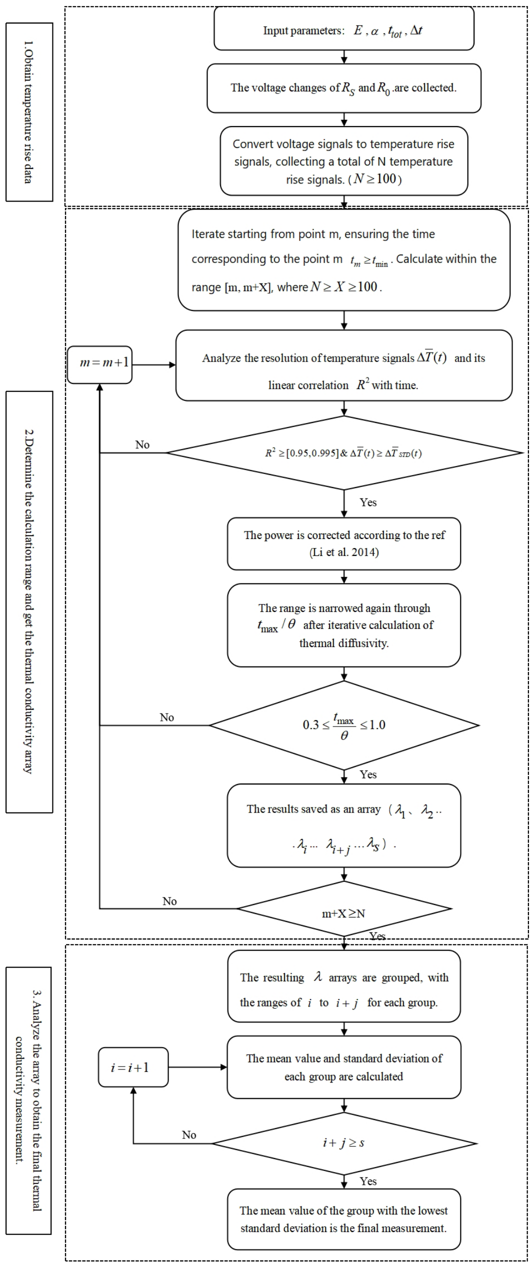

FIGURE 3. Flow chart of automatic algorithm for measuring thermal conductivity with TPS

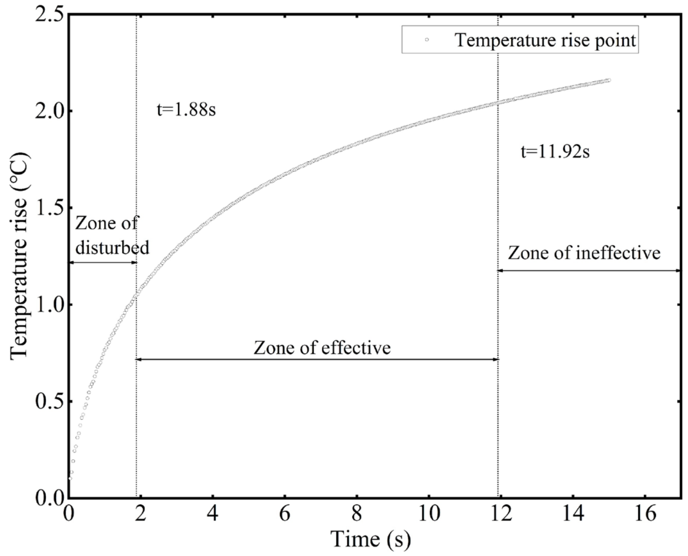

FIGURE 4. Temperature rise curve division of stainless-steel when P=2.5W (Zone of disturbed represents that the selected data are influenced by other factors; Zone of measurement represents the selected data are effective for calculating the thermal conductivity; Zone of the ineffective represents the resolution of the selected data is too lower)

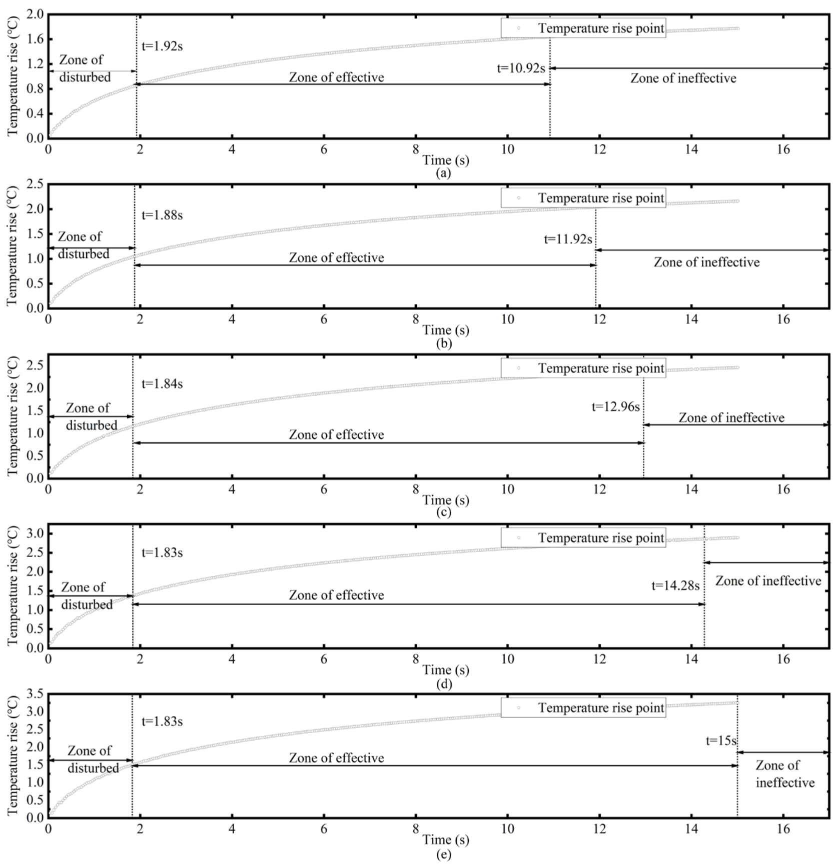

FIGURE 5. Variation of measurement intervals division with power (a) 2.1W, (b) P=2.5W, (c) P=3W, (d) P=3.5W, and (e) P=4.0W

TABLE 2. Length of stainless-steel measuring intervals varies with power

Power/W	Disturbed interval length/s	Effective interval length/s	Ineffective interval length/s	Effective interval length ratio/%
2.1	1.92	9	4.08	60
2.5	1.88	10.04	3.08	66.95
3.0	1.84	11.08	3.92	74.0
3.5	1.83	12.45	0.72	83.0
4.0	1.83	13.17	0	87.8

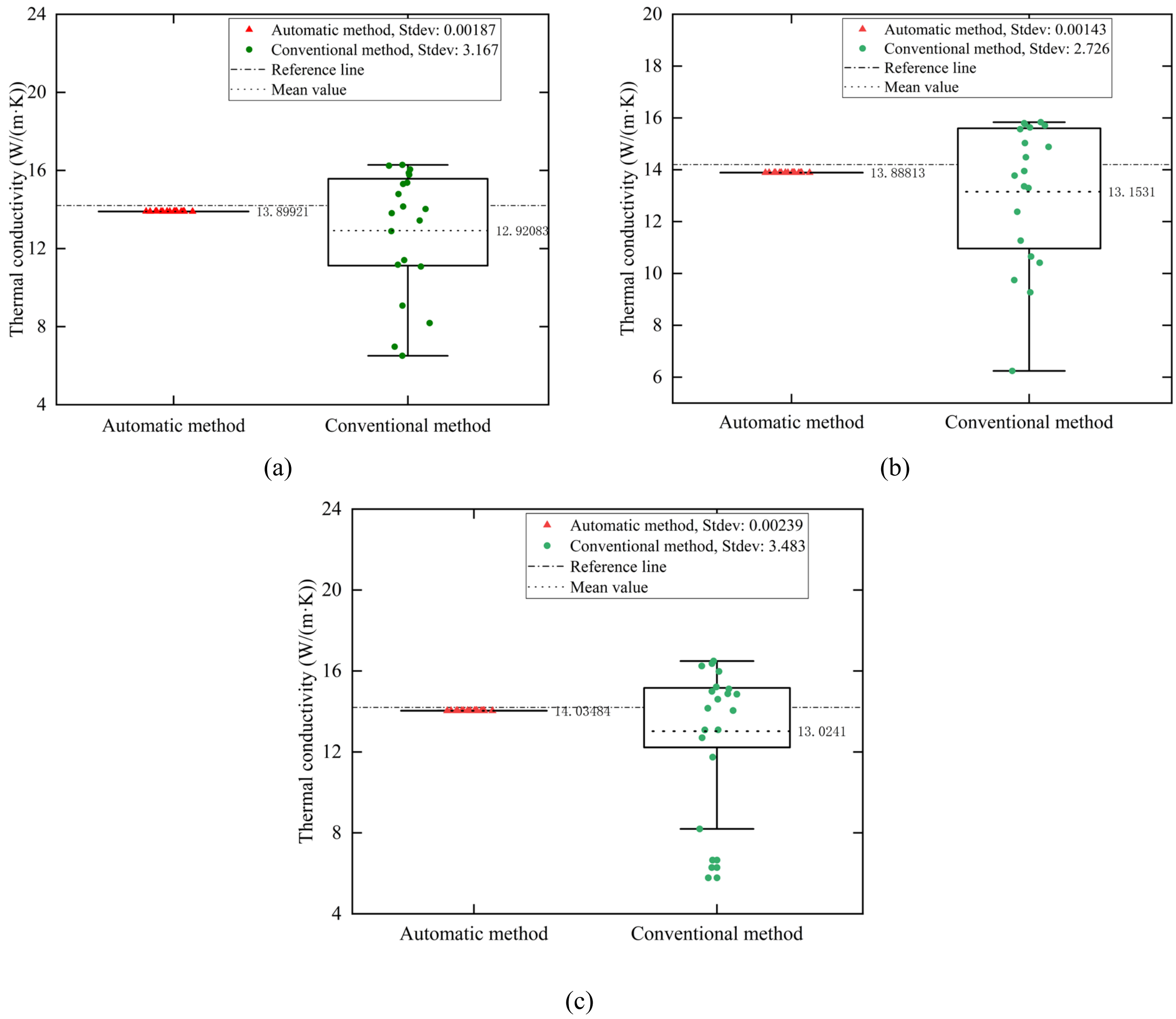

FIGURE 6. Thermal conductivity measurement results of stainless-steel using automatic and conventional methods at different powers (a) P=2.1W, (b) P=2.5W, and (c) P=3.0W

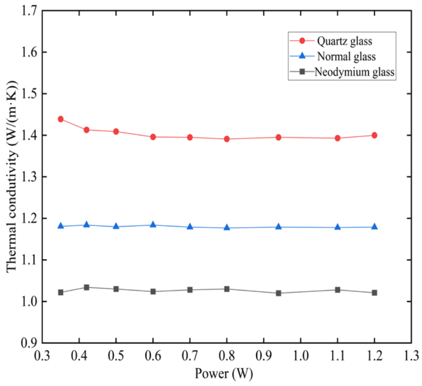

(a)

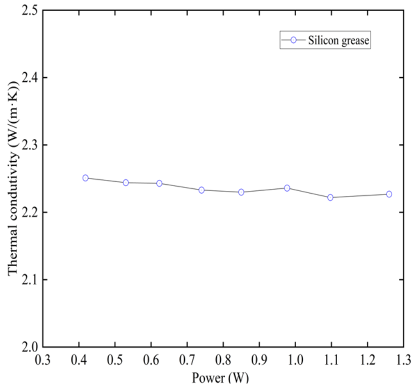

(b)

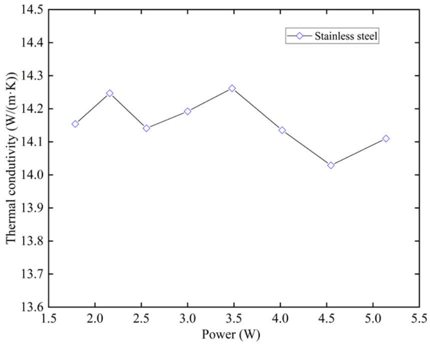

(c)

FIGURE 7. Five kinds of materials thermal conductivity distribution with power (a) Neodymium glass, ordinary glass, quartz glass, (b) Heat dissipation silicone grease, and (c) Stainless-steel

TABLE 3. Measured values and reference values of five materials

Material	λ_{TPS} /Wm^{-1}K^{-1}	λ_{THW} /Wm^{-1}K^{-1}	λ_0 /Wm^{-1}K^{-1}	ε /%
Neodymium glass	1.026	0.991	-	3.5
Ordinary glass	1.180	1.176	-	0.3
Quartz glass	1.403	-	1.42	1.1
Heat dissipation silicone grease	2.236	2.215	-	0.94
Stainless-steel	14.159	-	14.2	0.29

stainless-steel. The mean value and deviation are provided in Table 3, where λ_{THW} denotes value measured by the hot-wire measuring instrument, λ_0 is the calibration value, λ_{TPS} represents value measured by the TPS method, and ε indicates the deviation between the measured and reference value.

Table 3 shows the deviations between measurements and reference for five materials are all within 5%, indicating that the TPS measurement platform built in this experiment is highly accurate. Combined with the distribution of thermal conductivity of various materials with respect to power as shown in Figure 7, it can be concluded that the algorithm proposed in this paper exhibits good stability, high precision, and slight variation of measurement results with power.

CONCLUSION

This study has proposed an automatic algorithm that can exclude disturbing and ineffective data points, in which case the measurement of thermal conductivity is more accurate with good reproductivity than traditional methods.

The measurement of five different samples proves that the errors can keep in 4% by this new algorithm, and the standard deviations are also reduced. By measuring the stainless-steel sample with various powers, it confirms that the measurement accuracy tends to be improved with higher heating power for traditional methods. This is because the effect of contact thermal resistance is reduced with much more obvious temperature rise, and the analysis interval could be easily distinguished. However, many low thermal conductivity materials are not suitable for high power measurements. In comparison, with automatically selecting effective analysis interval among data points, the developed algorithm gives more objective thermal conductivity results which are less affected by external environment, such as the difference in operation habits and applied heating powers.

ACKNOWLEDGEMENTS

The authors are grateful for the financial supports by the Scientific project of China Manned Space (No. YYMT1201-EXP02), National Science Foundation of China (grant nos. 52072385 and 51606209), and Shanghai Technical Platform for Testing and Characterization on Inorganic Materials (grant no.14DZ2292900). The authors declare that they have no known competing financial interests or personal relationships that could have appeared to influence the work reported in this paper.

REFERENCES

Ai, Q., Hu, Z-W., Liu, M., Xia, X-L. & Xie, M. 2016. Influence of sensor orientations on the thermal conductivity measurements of liquids by transient hot disk technique. *Journal of Thermal Analysis and Calorimetry* 128: 289-300.

Almanza, O., Rodríguez-Pérez, M.A. & De Saja, J.A. 2004. Applicability of the transient plane source method to measure the thermal conductivity of low-density polyethylene foams. *Journal of Polymer Science Part B: Polymer Physics* 42(7): 1226-1234.

Assael, M.J., Antoniadis, K.D. & Wakeham, W.A. 2010. Historical evolution of the transient hot-wire technique. *International Journal of Thermophysics* 31(6): 1051-1072.

Assael, M.J., Antoniadis, K.D. & Tzetzis, D. 2008. The use of the transient hot-wire technique for measurement of the thermal conductivity of an epoxy-resin reinforced with glass fibres and/or carbon multi-walled nanotubes. *Composites Science and Technology* 68(15-16): 3178-3183.

Assael, M.J., Dix, M., Gialou, K., Vozar, L. & Wakeham, W.A. 2002. Application of the transient hot-wire technique to the measurement of the thermal conductivity of solids. *International Journal of Thermophysics* 23(3): 615-633.

Bohac, V., Gustavsson, M.K., Kubicar, L. & Gustafsson, S.E. 2000. Parameter estimations for measurements of thermal transport properties with the hot disk thermal constants analyzer. *Review of Scientific Instruments* 71(6): 2452-2455.

Cahill, D.G. 1990. Thermal conductivity measurement from 30 to 750 K: the 3ω method. *Review of Scientific Instruments* 61(2): 802-808.

Elkholy, A., Sadek, H. & Kempers, R. 2019. An improved transient plane source technique and methodology for measuring the thermal properties of anisotropic materials. *International Journal of Thermal Sciences* 135: 362-374.

Gustafsson, S.E. 1991. Transient plane source techniques for thermal conductivity and thermal diffusivity measurements of solid materials. *Review of Scientific Instruments* 62(3): 797-804.

Gustavsson, M., Karawacki, E. & Gustafsson, S.E. 1994. Thermal conductivity, thermal diffusivity, and specific heat of thin samples from transient measurements with hot disk sensors. *Review of Scientific Instruments* 65(12): 3856-3859.

Huang, L-P. 2007. Verification of the measurement accuracy and the test range of thermophysical properties of transient plane source (TPS) method. *Journal of Astronautic Metrology* 26(4): 25-29.

Huang, L. & Liu, L-S. 2009. Simultaneous determination of thermal conductivity and thermal diffusivity of food and agricultural materials using a transient plane-source method. *Journal of Food Engineering* 95(1): 179-185.

ISO 2008 Plastics - determination of thermal conductivity and thermal diffusivity - Part 2: Transient plane heat source (hot disc) method ISO 22007-2 (Geneva: ISO).

Kim, K., Lee, J. & Koo, J. 2019. Automated thermal conductivity measurement algorithm for the transient hot wire method. *Journal of Mechanical Science and Technology* 33(6): 3001-3009.

Li, Y., Shi, C., Liu, J., Liu, E., Shao, J., Chen, Z., Dorantes-Gonzalez, D.J. & Hu. X. 2014. Improving the accuracy of the transient plane source method by correcting probe heat capacity and resistance influences. *Measurement Science and Technology* 25: 015006.

Lian, T-W., Kondo, A., Akoshima, M., Abe, H., Ohmura, T., Tuan, W-H. & Naito, M. 2016. Rapid thermal conductivity measurement of porous thermal insulation material by laser flash method. *Advanced Powder Technology* 27(3): 882-885.

Ma, A., Cai, C., Yang, J. & Zhou, T. 2021. Measuring thermophysical properties of building insulation materials using transient plane heat source method. *Energy and Buildings* 240: 110819.

Malinarič, S. & Dieška, P. 2015. Concentric circular strips model of the transient plane source-sensor. *International Journal of Thermophysics* 36(4): 692-700.

Mo, S., Hu, P., Cao, J., Chen, Z., Fan, H. & Yu, F. 2006. Effective thermal conductivity of moist porous sintered nickel material. *International Journal of Thermophysics* 27(1): 304-313.

Nagai, H., Mamiya, M. & Okutani, T. 2007. Thermal conductivity measurement of molten indium antimonide using hot-disk method in short-duration microgravity. *Japanese Journal of Applied Physics* 46(12): 7920-7924.

Wang, H., Ihms, D.W., Brandenburg, S.D. & Salvador, J.R. 2019. Thermal conductivity of thermal interface materials evaluated by a transient plane source method. *Journal of Electronic Materials* 48(7): 4697-4705.

Warzoha, R.J. & Fleischer, A.S. 2014a. Determining the thermal conductivity of liquids using the transient hot disk method. Part I: Establishing transient thermal-fluid constraints." *International Journal of Heat and Mass Transfer* 71: 779-789.

Warzoha, R.J. & Fleischer, A.S. 2014b. Determining the thermal conductivity of liquids using the transient hot disk method. Part II: Establishing an accurate and repeatable experimental methodology. *International Journal of Heat and Mass Transfer* 71: 790-807.

Xamán, J., Lira, L. & Arce, J. 2009. Analysis of the temperature distribution in a guarded hot plate apparatus for measuring thermal conductivity. *Applied Thermal Engineering* 29(4): 617-623.

Zhang, H., Li, Y-M. & Tao, W-Q. 2017. Theoretical accuracy of anisotropic thermal conductivity determined by transient plane source method. *International Journal of Heat and Mass Transfer* 108: 1634-1644.

Zhang, H., Jin, Y., Gu, W., Li, Z.Y. & Tao, W.Q. 2013. A numerical study on the influence of insulating layer of the hot disk sensor on the thermal conductivity measuring accuracy. *Progress in Computational Fluid Dynamics* 13(3-4): 191-201.

Zhao, W., Yang, Y., Bao, Z., Yan, D. & Zhu, Z. 2020. Methods for measuring the effective thermal conductivity of metal hydride beds: A review. *International Journal of Hydrogen Energy* 45(11): 6680-6700.

Zheng, Q., Kaur, S., Dames, C. & Prasher, R.S. 2020. Analysis and improvement of the hot disk transient plane source method for low thermal conductivity materials. *International Journal of Heat and Mass Transfer* 151: 119331.

*Corresponding author; email: zzhchen@usst.edu.cn